Sliding mode control of a PMSM railway traction drive fed by multi-level inverter

Vo Thanh Ha[1], Vo Quang Vinh[2]
[1]Department of Cyberntics, Faculty of Electrical and Electronic Engineering, University of Transport and Communications, Hanoi City, Viet Nam
[2]Faculty of Control and Automation, Electric Power University, Hanoi City, Viet Nam

Article Info	ABSTRACT
	This work offers the sliding mode control (SMC) based control scheme for a railway traction transmission system fed by a five-level T-type inverter. This nonlinear control approach is created for the speed and torque loop control of the permanent magnet synchronous motor (PMSM) railway traction drive system supplied by a multi-level inverter. The article also includes a mathematical model of a PMSM motor and torque load to design controllers. The paper expressed the vector voltage modulation design incorporating a five-level T-Type inverter. The research proposes a control scheme for the railway traction drive system that enhances transmission quality by lowering the torque ripper and stator current harmonic distortion and extending converter life. Through MATLAB simulation, the study findings are validated. *This is an open access article under the [CC BY-SA](#) license.*
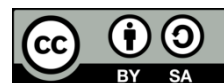
Corresponding Author:

Vo Thanh Ha
Department of Cyberntics, Faculty of Electrical and Electronic Engineering
University of Transport and Communications
No. 3 CauGiay District, Hanoi City, Viet Nam
Email: vothanhha.ktd@utc.edu.vn

1. INTRODUCTION

Nowadays, permanent magnet synchronous motors (PMSMs) are often utilized in electric vehicles and railway traction drives (RTDs) [1]-[3]. According to Ha *et al*. [4], Kuntanapreeda [5] study, this motor generates torque to extend the operating speed range. Moreover, it has features compatible with vehicle transmission's mechanical aspects, such as regenerative braking. On the other hand, the PMSM railway traction system often uses the field-oriented control (FOC) approach [6]. Consequently, the FOC reduces the usage of torque ripper and torque closed-loop control in railway trains. The regulated PMSM drive mechanism is very efficient [7]. However, PMSM motors can produce resistance torque when the motor is operating. The resistance torque will restrict the engine's ability to promote sufficient torque and speed [8], [9]. This issue will be resolved using the maximum torque per ampere (MPTA) approach. The MPTA has a feature to generate the best torque for the PMSM at a particular phase current. MTPA control maintains a specific torque angle between the positive d-axis and the current phase in the d-q frame [10]-[13].

The speed and torque loops are often controlled by cascading the traction vector control architecture. These controllers are refined and upgraded to provide various control strategies' torque and speed responses. The control methods are proportional integral (PI), active disturbance rejection control (ADRC), ADRC, deadbeat, backstepping, flatness, passive, and sliding mode control. These control approaches have advocated the benefits of a more comprehensive speed range, little harmonic distortion, and no overturning [14]-[16]. For instance, the PI control approach provides quick and easy design benefits, but

when disturbed, the torque and speed response is simple to alter [17]. Providing a solid assurance for the necessary answers is the rolling control approach. This approach is still in use. However, it is still susceptible to motor parameter changes and system noise [18]. In particular, the sliding mode control stabilizes the system following the chosen sliding surface, addressing the sensitivity to motor settings and many other problems. In addition, the sliding control design is thoroughly and clearly shown using mathematical calculations. According to the Lyapunov theorem of [19]-[21] documents, the traction drive system is stabilized. This article will be presented sincerely with the sliding mode control design for speed and torque loop control. This technique reduces torque ripper, and the railway traction drive system operates steadily over the whole speed range.

Additionally, it enhances torque response to fulfill demands for speed and precision. Space vector modulation (SVM) for a five-level T-type inverter will be discussed in this post. In terms of transistor valve switching frequency, harmonic distortion, and converter life, this multi-level inverter is superior to other structural two-level and multi-level inverters, claims the paper [22]-[26]. Table 1 displays these ratings.

Table 1 demonstrates that the T-type multi-level inverter has the advantage of decreasing the number of semiconductor valves and capacitors while increasing the voltage level. The study is organized as: First, section 1 the introduction expresses the reason for the slide mode controller application of a PMSM railway traction drive fed by a multi-level inverter. Second, the PMSM motor and load mathematical model is presented in section 2. Third, a detailed explanation of 5-level voltage vector modulation will be provided in section 3. Fourth, the sliding mode control (SMC) method for the speed and torque loops is under control in section 4. Section 5 will present the simulation results and a short assessment of the suggested railway traction drive system's control structure. Finally, conclusion in section 6.

Table 1. Comparing multi-level inverter structures

Structure	Neutral point clamped (NPC)	Flying capacitor (FC)	Cascaded H-bridge (CHB)	T−Type
Valve number insulated gate bipolar transistor (IGBT)	24	24	24	9
Valve number diode	24	24	0	0
Clamp diode	36	0	0	0
Number of capacitors	4	4	6	0

2. MATHEMATICAL MODEL OF A PMSM MOTOR AND TORQUE LOAD
2.1. The mathematical mode of a PMSM motor
Based on the documentation [27], the PMSM's mathematical model is as follows since the FOC technique is utilized to govern it.

$$\begin{cases} u_{sd} = L_{sd} \frac{di_{sd}}{dt} + R_s i_{sd} - \omega L_{sq} i_{sq} \\ u_{sq} = L_{sq} \frac{di_{sq}}{dt} + R_s i_{sq} + \omega L_{sd} i_{sd} + \omega\psi \end{cases} \tag{1}$$

Where: i_{sd}, i_{sq} are dq components of the stator current; u_{sd}, u_{sq} are dq components of the stator voltage; L_{sd}, L_{sq} are dq components of stator inductance, ω is mechanical speed; ψ is rotor flux; z_p is number of poles. The following is a description of the motor's torque calculation in (2):

$$T_M = \frac{3}{2} z_p [\psi i_{sq} + (L_{sd} - L_{sq}) i_{sd} i_{sq}] \tag{2}$$

The equation represents the PMSM's mechanical in (3):

$$T_M = T_L + \frac{J d\omega}{dt} \tag{3}$$

Where: T_M, T_T are motor and load torques; J is inertia torque.

2.2. Mathematical model of load torque
The load torque is the total of the forces that oppose the motion of the railroad transmission motor. The following formula is used to compute the load mode:

$$F(t) = a_{11} M + a_{12} n + a_2 M v(t) + a_3 A k v(t)^2 + M g \sin \alpha \tag{4}$$

Where, M, n, A, k, α represent the weight of the train, the shaft, the surface area in the direction of displacement, the track and gear parameters; v is train speed.

3. THE SMC CONTROLER DESIGN OF SPEED AND TORQUE CONTROL LOOPS
3.1. Speed controller

The SMC is an efficient tool for nonlinear systems, load torque disturbances, and parameter variation changes. The steps that the speed control for a railroad traction motor is intended to take are:

$$\dot{\omega} + \frac{1}{J}T_L = \frac{1}{J}T_M \tag{5}$$

Where: $T_m = \frac{3}{2}\frac{L_m^2}{L_r}p\psi_{rd}\frac{i_{sq}}{L_m} = k_\omega i_{sq}; k_\omega = \frac{3}{2}\frac{L_m}{L_r}p\psi_{rd}$ $a = \frac{T_L}{J}; b = \frac{k_\omega}{J}$

The speed error can be determined as:

$$e(t) = \omega(t) - \omega^*(t)\Delta b \tag{6}$$

Next, the sliding surface variable $s(t)$:

$$s(t) = e(t) - \int_0^t (k-c)e(t)dt = 0 \tag{7}$$

With c is a typical motion under sliding mode control to error to zero for all times. The variable structure speed controller is designed as:

$$u(t) = ke(t) - \beta \, sgn(s) \tag{8}$$

The gain defined before with k is $k < 0$ to $(k-c) < 0$. The switching gain, β, must be selected to $\beta \geq d(t)$, $sgn(.)$ is the switching function. Then, defining Lyapunov function and derivate it. As shown in (9):

$$V(t) = \frac{1}{2}s(t)s(t) \tag{9}$$

The derivative (10) is then calculated as:

$$\dot{V}(t) = s[d - \beta \, sgn(s) + ce] < 0 \tag{10}$$

In (10) $\dot{V}(t) < 0$, that is, the SMC design and SMC circumstances. Consequently, the system's SMC may be calculated as:

$$i^*_{sq}(t) = i_{sq}(t) = \frac{1}{b}[ke - \beta \, sgn(s) + a + \dot{\omega}^*] \tag{11}$$

3.2. Torque controller

The SMC is designed to generate the rotor voltage reference from the torque and flux vector:

$$s_T = e_T = T_m^* - T_m \tag{12}$$

$$s_\psi = e_\psi = \psi^* - \psi \tag{13}$$

From (12) and (13) can be written by matric:

$$\begin{bmatrix} \dot{s}_T \\ \dot{s}_\psi \end{bmatrix} = -\begin{bmatrix} 3/2z_p(L_{sd}i_{sq} - L_{sq}i_{sq}) & 3/2z_p[(L_{sd}i_{sd} - \psi) - L_{sq}i_{sd}] \\ (L_{sq}i_{sq} - \psi)L_{sd} & L_{sq}^2 i_{sq} \end{bmatrix}\begin{bmatrix} i_{sd} \\ i_{sq} \end{bmatrix} \tag{14}$$

Where:

$$K = \begin{bmatrix} 1.5z_p(L_{sd}i_{sq} - L_{sq}i_{sq}) & 1.5z_p[(L_{sd}i_{sd} - \psi) - L_{sq}i_{sd}] \\ (L_{sd}i_{sd} - \psi)L_{sd} & L_{sq}^2 i_{sq} \end{bmatrix}; A = \begin{bmatrix} \frac{-R_s}{L_{sd}} & z_p\omega \\ \frac{-R_s}{L_{sd}} & \frac{-R_s}{L_{sq}} \end{bmatrix}; B = \begin{bmatrix} \frac{1}{L_{sd}} & 0 \\ 0 & \frac{1}{L_{sq}} \end{bmatrix} H = \begin{bmatrix} 0 \\ \frac{z_p\psi}{L_{sq}} \end{bmatrix}$$

In (14) can be written:

$$\begin{bmatrix} \dot{s}_T \\ \dot{s}_\psi \end{bmatrix} = -K(A \begin{bmatrix} i_{sd} \\ i_{sq} \end{bmatrix} + B \begin{bmatrix} u_{sd} \\ u_{sq} \end{bmatrix} + H) \tag{15}$$

Control variable for torque and flux can be calculated from (15):

$$\begin{bmatrix} u_{sd}^* \\ u_{sq}^* \end{bmatrix} = B^{-1}(K^{-1} \begin{bmatrix} l_{11} & l_{12} \\ l_{21} & l_{22} \end{bmatrix} \begin{bmatrix} s_T & s_\psi \\ sgn(s_T) & sgn(s_\psi) sgn \end{bmatrix} - A \begin{bmatrix} i_{sd} \\ i_{sq} \end{bmatrix} - H) \tag{16}$$

The sliding face is choice as shown:

$$\begin{cases} \dot{s}_T = -l_{11}s_T - l_{12} \, sgn(s_T) \\ \dot{s}_\psi = -l_{12}s_\psi - l_{22} \, sgn(s_\psi) \end{cases} \tag{17}$$

The stability research provided an application of the Lyapunov approach. Regarding the potential Lyapunov function:

$$V(t) = \frac{1}{2}s(t)s(t) \tag{18}$$

The derivative (18) is then calculated as:

$$\dot{V} = -s_T(l_{11}s_T + l_{12}sgn(s_T)) - s_\psi(k_{21}s_\psi + l_{22}sgn(s_\psi)) \tag{19}$$

The derivative (19) can be written as shown:

$$\dot{V} = -[(l_{11}s_T^2 + l_{12}|s_T|) + (l_{21}s_\psi^2 + l_{22}|s_\psi|] \tag{20}$$

with l_{ij} are positive gain if $\dot{V} < 0$, then the torque response is established sustainably.

4. MODULATION FOR *T*-TYPE 5-LEVEL INVERTER

Based on Ha *et al.* [22], structure for a *T*-type 5-level inverter is shown Figure 1. This *T*-type inverter has 5-level: ½ V_{dc}, $- V_{dc}$, 0, $+ ½ V_{dc}$, $+ V_{dc}$. (V_{dc} is DC voltage). The *T*-type 5-level inverter is modulated by space vector modulation (SVM). Implementation SVMs steps:

Step 1: from modulation voltage, convert the coordinate system from abc to $\alpha\beta$.
Step 2: from $\alpha\beta$ to g, h coordinate system.
Step 3: determine the sector position of the modulation vector.
Step 4: determine the modulation period for the vector.
Step 6: determine the switching state.
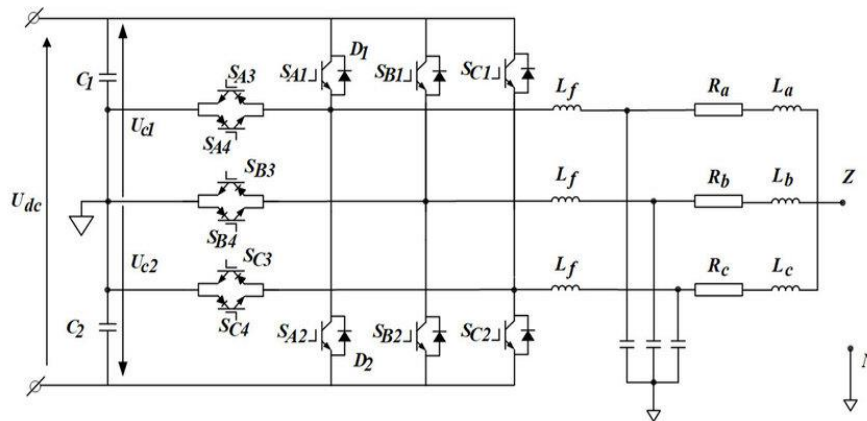Step 7: pulse the valve.

Figure 1. A *T*-type 5-level inverter structure

The space vector 3-phase 5-level is shown in Figure 2, [22]. It can be seen in Figure 1 that, for an n-level 3-phase converter, the number of switching states will be n^3, and there are $6x(n-1)^2$ triangles in the spatial vector diagram. Thus, for a 5-level T-type inverter, the number of switching states will be 5^3, and there are 72 triangles in the space vector diagram. Table of state vectors in sectors is shown at Table 2.
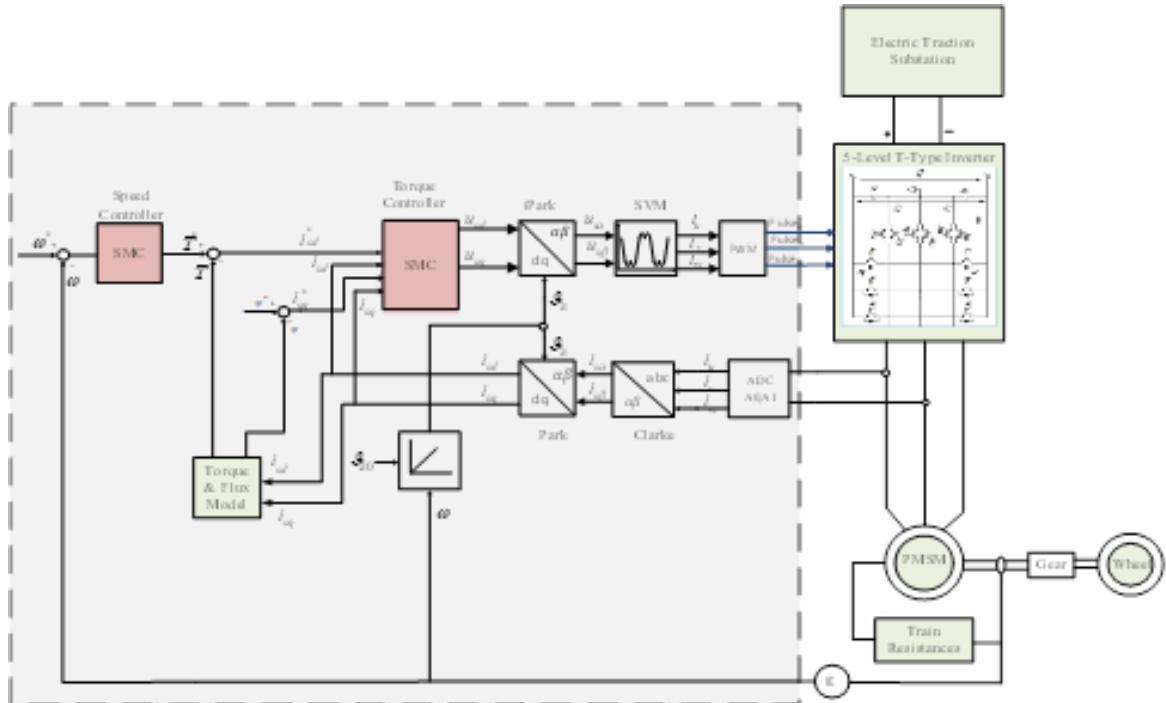

Figure 2. The structure of the SMC controllers combined the T-type 5 level inverter for RTD applications

Table 2. Table of state vectors in sectors

State vector	I	II	III	IV	V	VI
$\begin{bmatrix} k_{ix} \\ k_{iy} \end{bmatrix}$	$\begin{bmatrix} (k_A - k_B) \\ (k_B - k_C) \end{bmatrix}$	$\begin{bmatrix} (k_A - k_C) \\ (k_B - k_A) \end{bmatrix}$	$\begin{bmatrix} (k_B - k_C) \\ (k_C - k_A) \end{bmatrix}$	$\begin{bmatrix} (k_B - k_A) \\ (k_C - k_B) \end{bmatrix}$	$\begin{bmatrix} (k_C - k_A) \\ (k_A - k_B) \end{bmatrix}$	$\begin{bmatrix} (k_C - k_B) \\ (k_A - k_C) \end{bmatrix}$
$\begin{bmatrix} k_A \\ k_B \\ k_C \end{bmatrix}$	$\begin{bmatrix} k \\ k - k_{1x} \\ k - k_{1s} \end{bmatrix}$	$\begin{bmatrix} k - k_{2y} \\ k \\ k - k_{2s} \end{bmatrix}$	$\begin{bmatrix} k - k_{3s} \\ k \\ k - k_{3x} \end{bmatrix}$	$\begin{bmatrix} k - k_{4s} \\ k - k_{4y} \\ k \end{bmatrix}$	$\begin{bmatrix} k - k_{5x} \\ k - k_{5s} \\ k \end{bmatrix}$	$\begin{bmatrix} k \\ k - k_{6s} \\ k - k_{6y} \end{bmatrix}$

5. RESULTS AND DISCUSSION

The control structure of 5 level T-type inverter for railway traction motor is presented in Figure 2. Simulation with parameters of 5 level T-type inverter and PMSM's parameters used railway traction motor follow as Table 3. T-type inverter simulation parameters using SVM are expressed in Table 4.

Table 3. Simulation with PMSM's parameters used RTD

Parameters	Symbol	Value
DC voltage	U_{dc}	600
Frequency of modulation	fs	2000Hz
Power	P_{dm}	270 kW
Rated speed	n_{dm}	3000 rpm
Rated voltage	U_{dm}	400V
Pole pair	p	1
Power factor	$cos \varphi$	0.9
Stator resistance	R_s	0.0126 Ω
Rotor resistance	R_r	0.00865Ω
Rotor inductance	L_r	0.00822H
Mutual inductance	L_m	0.0088H
Voltage		750 VDC
Maximum speed for the train		80km/h

Table 4. Simulation parameters of T-type 5 level inverter

Power circuit	Parameter
DC capacitor C1	U_{dc}
DC capacitor C1	fs
Filter inductor Li	P_{dm}
DC voltage Vc	n_{dm}
Filter capacitor	U_{dm}
Pulse frequency	p

5.1. Evaluating results of T-type 5 level inverter

Character of the T-type 5 level inverter is evaluated based on output voltage responses and current harmonic distortion. The inverter output voltage response is shown in Figure 3. The current harmonic distortion is shown in Figure 4.
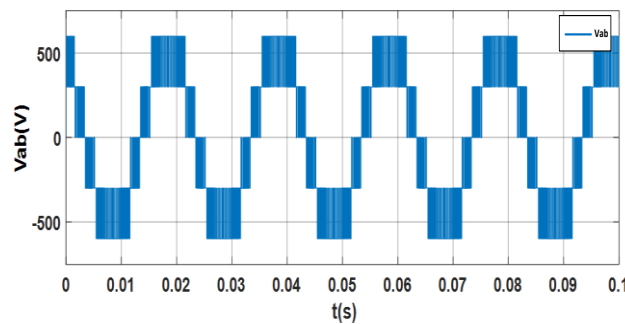
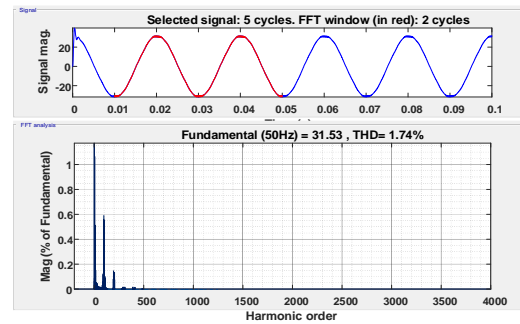Figure 3. The inverter output voltage response

Figure 4. The current harmonic distortion

Through simulation results of Figure 3 and Figure 4, there are some results as shown:
a. The inverter output voltage has the form of 5 levels, with an amplitude of 600 V
b. Sine wave output current with low harmonic distortion THD=1.74%
c. DC voltage on two unbalanced capacitors, with maximum difference up to ΔV_{cmax}=20 V (6%)

5.2. Evaluating results of the SMC controller

Case 1: the railway traction drive system is fed by a 5-level T-type inverter to simulate and evaluate the SMC controller in the traction drive system. Through the modeling of the given situation, some typical functioning RTMs are:
a. From $t = 0.5\ s$ to $t = 2.5\ s$, the PMSM motor is operating at pull process with parameters: $t_{1s} = 0\ (km/h)$; $t_{2s} = 30\ (km/h)$; $t_{3s} = 60\ (km/h)$
b. From $t = 2.5\ s$ to $t = 5.5\ s$, the PMSM motor is operating at coasting process with parameters: $t_{6s} = 50\ (km/h)$.
c. From $t = 6\ s$ to $t = 8\ s$, the PMSM motor is operating at braking process with parameters: $t_{7s} = 10\ (km/h)$; $t_{8s} = 0\ (km/h)$.

Simulation results in case 1 are shown in Figure 5. Figure 5(a) shows the speed responses of SMC and PI controllers, Figure 5(b) conveys torque responses of SMC and PI controllers, and Figure 5(c) displays the total harmonic distortion (THD) of a T-type 5-level inverter of SMC and PI controllers.

Based on the simulation results of Figure 5(a) and Figure 5(b), it is found that the SMC controller design for torque and speed controller has more advantages than the PI controller. The actual speed matches the reference speed with a fast set time. The ripple torque is small with ΔT_M=10%. Meanwhile, the PI controller's ripple torque is still high ΔT_M%=20%. Therefore, the T-type 5-level inverter is torque-ripper-reduced. Moreover, in the research to ensure low THD and low ripple torque. In addition, the simulation results of Figure 5(c) show the THD for the T-type 5 level inverter combined SMC controller with THD=3.89%. In contrast, the PI controller structure combined with the multi-level inverter results in a THD of 6.58%, much higher than the proposed control structure.

Case 2: to showcase the reliability of the railway traction drive system, the paper used an example where the rotor resistance raised by 50%. Through the simulation of the following scenario, some typical working RTM are just as:

a. From $t = 0.5\,s$ to $t = 3\,s$, the PMSM motor is working following parameters in a pull process: $t_{1s} = 0\ (km/h)$; $t_{2s} = 40\ (km/h)$; $t_{3s} = 70\ (km/h)$.
b. From $t = 3\,s$ to $t = 6\,s$, the PMSM is operating at coasting process with parameters: $t_{6s} = 60\ (km/h)$.
c. From $t = 6\,s$ to $t = 8\,s$, the IM is operating at braking process with parameters: $t_{7s} = 5\ (km/h)$; $t_{8s} = 0\ (km/h)$.
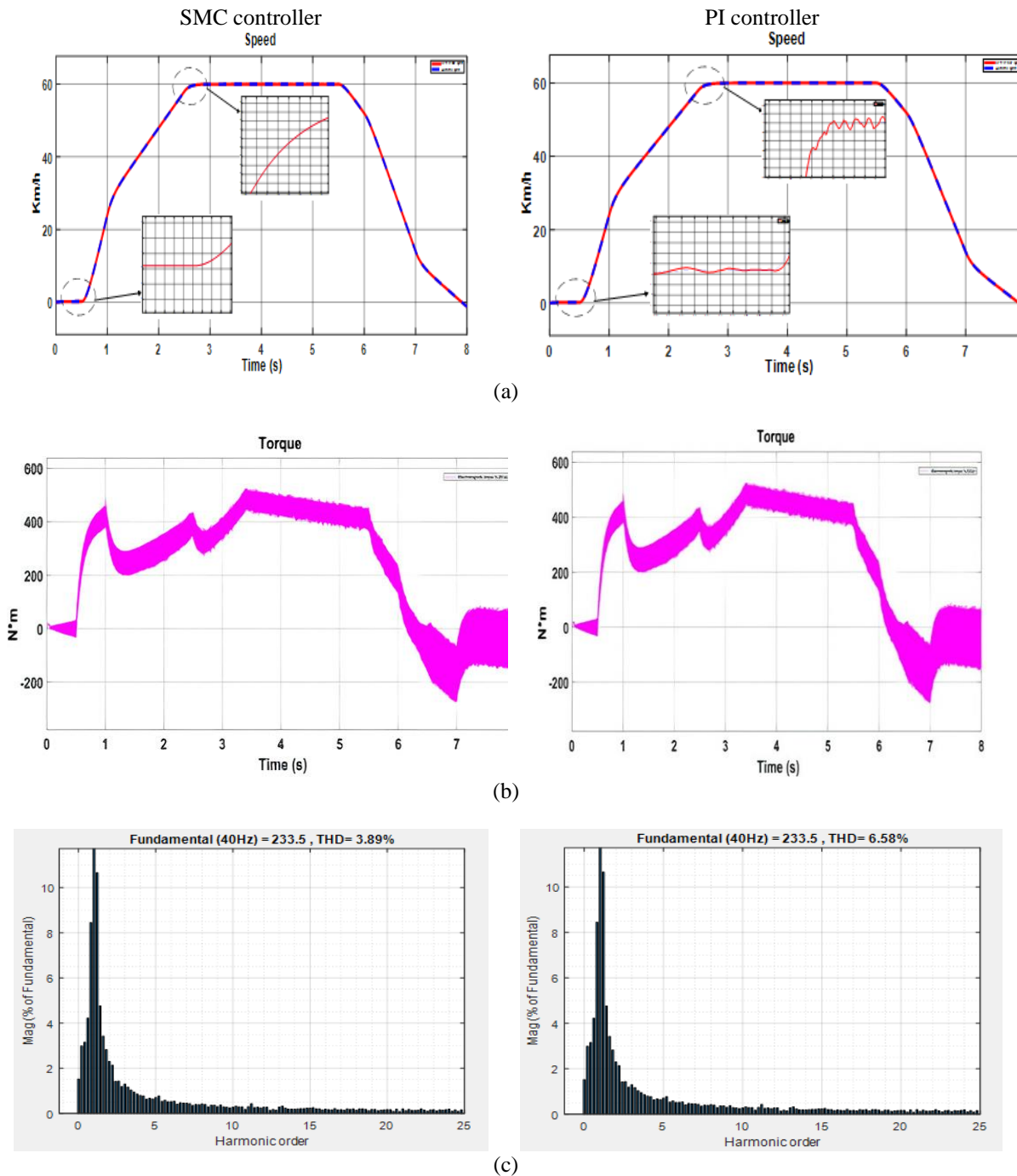

(a)

(b)

(c)

Figure 5. The railway traction drive system fed by a 5-level T-type inverter with constant rotor resistance analysis with of: (a) speed responses of SMC and PI controllers, (b) torque responses of SMC and PI controllers, and (c) the THD of a T-type 5-level inverter of SMC and PI controllers

Simulation results for the railway traction drive system fed by a 5-level T-type inverter with rotor resistance increasing to 50% are shown in Figure 6. Figure 6(a) shows the speed responses of SMC and PI

controllers, Figure 6(b) conveys torque responses of SMC and PI controllers, and Figure 6(c) displays the THD of a T-type 5-level inverter of SMC and PI controllers.

Based on the simulation findings in Figure 6(a) and Figure 6(b) for the SMC controller, the system was stable, with a rapid stabilization time and an actual speed that tracks the intended rate. Furthermore, the torque response is modest (20%). On the other hand, the simulation results of Figure 6(c) show that THD's 5-level inverter value rose to 3.93%, and the output voltage is in a sine wave shape. Meanwhile, the PI controller had a rate decrease at the speed setting step and had a significant ripple torque in the simulation results of Figure 6(a) and Figure 6(b) for the PI controller. THD's 5-level inverter value, on the other hand, rose to 12.55 % (Figure 6(c)).
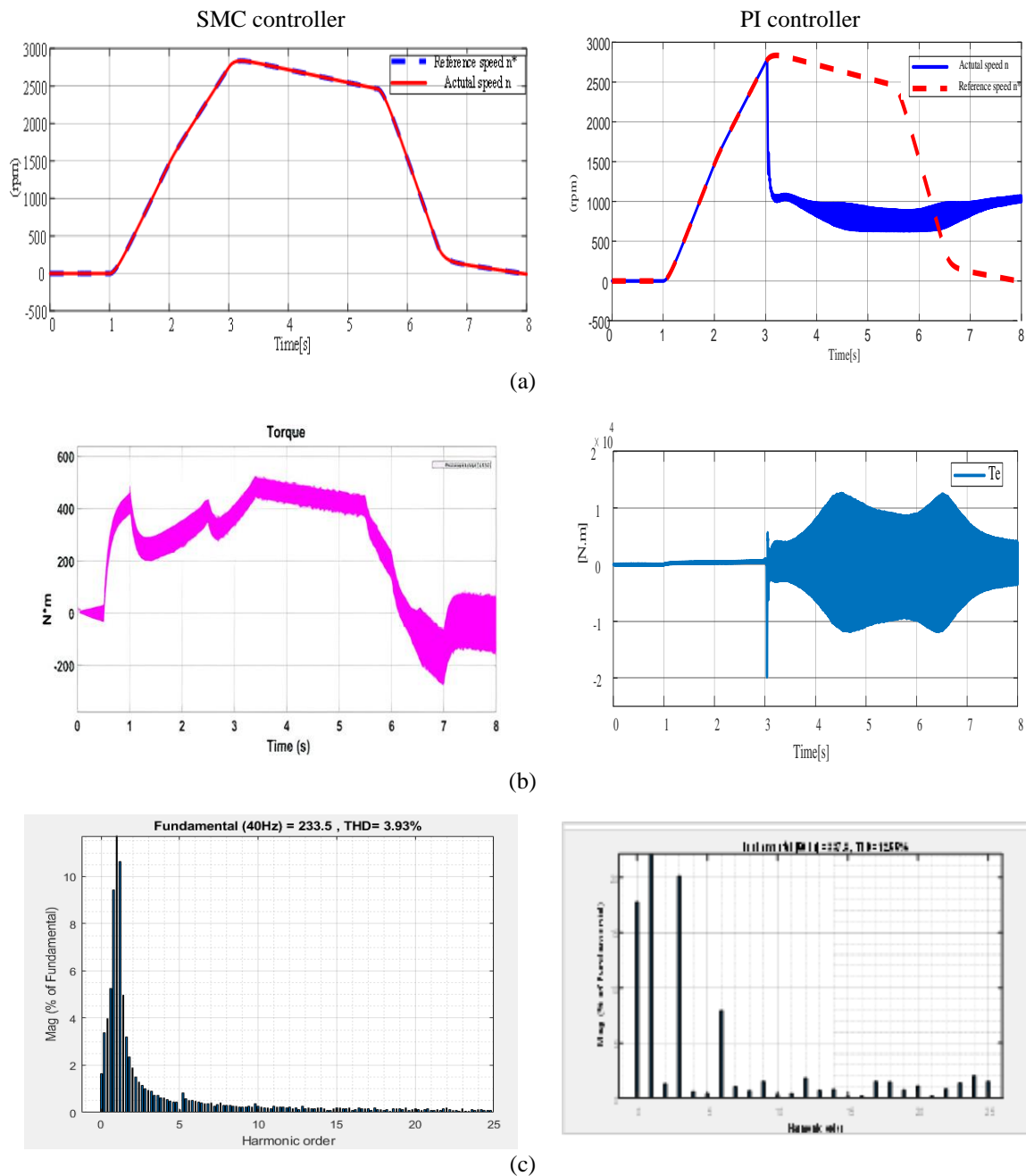

(a)

(b)

(c)

Figure 6. The railway traction drive system fed by a 5-level T-type inverter with rotor resistance increasing to 50% analysis with (a) speed responses of SMC and PI controllers; (b) torque responses of SMC and PI controllers of SMC and PI controllers; and (c) the THD of a T-type 5-level inverter of SMC and PI controllers

6. CONCLUSION

This paper proposes successfully researching a speed and torque controller using SMC control to control PMSMS motors fed by *T*-type multi-level inverters applied to railway traction drives. The simulation results proved that the multi-level inverter gave a sinusoidal phase voltage response, and the current harmonic distortion was slight. Furthermore, with the advantage of the *T*-type multi-level inverter, the speed and torque loop SMC controller achieves such achievements as the small torque ripper response and the required speed response. Responds to the necessary speed and torque even when system parameters change. However, the torque ripper still needs to be improved by intelligent controllers such as fuzzy combined with a neural or sliding mode controller connected with anti-vibration to strengthen and enhance this high-performance railway traction drive.

ACKNOWLEDGEMENTS

REFERENCES

[1] L. Frederick and G. K. Dubey, "AC motor traction drives - A status review," *Sadhana*, vol. 22, pp. 855-869, 1997. [Online]. Available: https://www.ias.ac.in/article/fulltext/sadh/022/06/0855-0869
[2] M. -Ş. Nicolae and I. -R. Bojoi, "A control strategy for an induction motor used for vehicular traction and/or positioning systems with variable speeds," *2012 International Conference on Applied and Theoretical Electricity (ICATE)*, 2012, pp. 1-6, doi: 10.1109/ICATE.2012.6403425.
[3] A. F. Abouzeid *et al.*, "Control Strategies for Induction Motors in Railway Traction Applications," *Energies*, vol. 13, no. 3, 2020, doi: 10.3390/en13030700.
[4] V. T. Ha, P. T. Giang, and P. Vu, "Multilevel inverter application for railway traction motor control," *Bulletin of Electrical Engineering and Informatics,* vol. 11, no. 4, pp. 1855-1866, 2022, doi: 10.11591/eei.v11i4.3964.
[5] S. Kuntanapreeda, "Traction Control of Electric Vehicles Using Sliding-Mode Controller with Tractive Force Observer," *International Journal of Vehicular Technology*," 2014, doi: 10.1155/2014/829097.
[6] S. K. Bade and V. A. Kulkarni, "Analysis of Railway Traction Power System Using Renewable Energy: A Review," *2018 International Conference on Computation of Power, Energy, Information and Communication (ICCPEIC)*, 2018, pp. 404-408, doi: 10.1109/ICCPEIC.2018.8525206.
[7] S. Nategh, D. Lindberg, R. Brammer, A. Boglietti, and O. Aglen, "Review and Trends in Traction Motor Design: Electromagnetic and Cooling System Layouts," *2018 XIII International Conference on Electrical Machines (ICEM)*, 2018, pp. 2600-2606, doi: 10.1109/ICELMACH.2018.8506817.
[8] Q. K. Nguyen, M. Petrich, and J. R. -Stielow, "Implementation of the MTPA and MTPV control with online parameter identification for a high speed IPMSM used as traction drive," *2014 International Power Electronics Conference (IPEC-Hiroshima 2014 - ECCE ASIA)*, 2014, pp. 318-323, doi: 10.1109/IPEC.2014.6869600.
[9] T -H. Liu, Y. Chen, M. -J. Wu, and B. -C Dai, "Adaptive controller for an MTPA IPMSM drive system without using a high-frequency sinusoidal generator," *The Journal of Engineering*, vol. 2017, no. 2, 2017, doi: 10.1049/joe.2016.0065.
[10] T. -H. Liu, S. -K. Tseng, and M. -B. Lu, "Auto-tuning flux-weakening control for an IPMSM drive system using a predictive controller," *2017 IEEE 26th International Symposium on Industrial Electronics (ISIE)*, 2017, pp. 238-243, doi: 10.1109/ISIE.2017.8001254.
[11] T. Sun, J. Wang, and X. Chen, "Maximum Torque Per Ampere (MTPA) Control for Interior Permanent Magnet Synchronous Machine Drives Based on Virtual Signal Injection," in *IEEE Transactions on Power Electronics*, vol. 30, no. 9, pp. 5036-5045, 2015, doi: 10.1109/TPEL.2014.2365814.
[12] K. Li and Y. Wang, "Maximum Torque Per Ampere (MTPA) Control for IPMSM Drives Based on a Variable-Equivalent-Parameter MTPA Control Law," in *IEEE Transactions on Power Electronics*, vol. 34, no. 7, pp. 7092-7102, 2019, doi: 10.1109/TPEL.2018.2877740.
[13] Y. A. -R. I. Mohamed and T. K. Lee, "Adaptive self-tuning MTPA vector controller for IPMSM drive system," in *IEEE Transactions on Energy Conversion*, vol. 21, no. 3, pp. 636-644, 2006, doi: 10.1109/TEC.2006.878243.
[14] V. T. Ha, N. T. Lam, V. T. Ha, and V. Q. Vinh, "Advanced control structures for induction motors with ideal current loop response using field oriented control," *International Journal of Power Electronics and Drive System (IJPEDS)*, vol. 10, no. 4, pp. 1758-1771, 2019, doi: 10.11591/ijpeds.v10i4.pp1758-1771.
[15] V. T. Ha, N. T. Lam, P. V. Tuan, and N. H. Quang, "Experiments Based Comparative Analysis of Nonlinear Speed Control Methods for Induction Motors," *Journal of Engineering and Technological Sciences*, vol. 53, no. 2, 2021, doi: 10.5614/j.eng.technol.sci.2021.53.2.12.
[16] R. D. Doncker, D. W. J. Pulle, and A. Veltman, "Advanced Electrical Drives: Analysis, Modeling, Control," *Power Systems*, London, New York: Springer, 2011, doi: 10.1007/978-94-007-0181-6.
[17] L. Wang, S. Chai, and D. Yoo, *PID and Predictive Control of Electrical Drives and Power*, Singapore: John Wiley & Sons, 2014, doi: 10.1002/9781118339459.
[18] J. Han, "From PID to Active Disturbance Rejection Control," in *IEEE Transactions on Industrial Electronics*, vol. 56, no. 3, pp. 900-906, 2009, doi: 10.1109/TIE.2008.2011621.
[19] K. Zhao, *et al.*, "Sliding mode-based velocity and torque controllers for permanent magnet synchronous motor drives system," *The Journal of Engineering, 7th International Symposium on Test Automation and Instrumentation (ISTAI 2018)*, 2019, vol. 2019, no. 23, pp. 8604-8608, doi: 10.1049/joe.2018.9065.
[20] M. S. Zaky, "Robust sliding mode speed controller-based model reference adaptive system (MRAS) and load torque estimator for Interior permanent magnet synchronous motor (IPMSM) drives," *Electric Power Components and Systems*, vol. 43, no. 13, pp. 1523–1533, 2015, doi: 10.1080/15325008.2015.1041624.
[21] J. Liu, H. Li, and Y. Deng, "Torque Ripple Minimization of PMSM Based on Robust ILC Via Adaptive Sliding Mode Control," in *IEEE Transactions on Power Electronics*, vol. 33, no. 4, pp. 3655-3671, 2018, doi: 10.1109/TPEL.2017.2711098.
[22] V. T. Ha, P. T. Giang, and V. H. Phuong, "T-Type Multi-Inverter Application for Traction Motor Control," *Engineering, Technology & Applied Science Research*, vol. 12, no. 2, pp. 8321-8327, 2022, doi: 10.48084/etasr.4776.

[23] J. Rodriguez, S. Bernet, B. Wu, J. O. Pontt, and S. Kouro, "Multilevel Voltage-Source-Converter Topologies for Industrial Medium-Voltage Drives," in *IEEE Transactions on Industrial Electronics*, vol. 54, no. 6, pp. 2930-2945, 2007, doi: 10.1109/TIE.2007.907044.

[24] H. Gupta, A. Yadav, and S. Maurya, "Dynamic performance of cascade multilevel inverter based STATCOM," *2016 IEEE 1st International Conference on Power Electronics, Intelligent Control and Energy Systems (ICPEICES)*, 2016, pp. 1-4, doi: 10.1109/ICPEICES.2016.7853479.

[25] P. Cortés, A. Wilson, S. Kouro, J. Rodriguez, and H. A. -Rub, "Model Predictive Control of Multilevel Cascaded H-Bridge Inverters," in *IEEE Transactions on Industrial Electronics*, vol. 57, no. 8, pp. 2691-2699, 2010, doi: 10.1109/TIE.2010.2041733.

[26] A. H. Ali, H. S. Hamad, and A. A. Abdulrazzaq, "An adaptable different-levels cascaded h-bridge inverter analysis for PV grid-connected systems," *International Journal of Power Electronics and Drive System*, vol. 10, no. 2, pp. 831-841, 2019, doi: 10.11591/ijpeds.v10.i2.pp831-841.

[27] N. P. Quang, J. -A. Dittrich, "Vectsor control of three-phase AC machines – System development in the practice", *2nd edition,* Berlin, Heidelberg: Springer, 2015. [Online]. Available: https://link.springer.com/book/10.1007/978-3-662-46915-6

BIOGRAPHIES OF AUTHORS

Vo Thanh Ha 🆔 🔍 SC ◑ is a lecturer in the Faculty of Electrical and Electrical Engineering, University of Transport and Communications. She received her B.S. in Control and Automation Engineering from the Thai Nguyen University of Technology, Vietnam, in 2002. She received her Master's degree from the Hanoi University of Science and Technology, Vietnam, in 2004. She received a Ph.D. in Control and Automation Engineering from the Hanoi University of Science and Technology, Vietnam, in 2020. Her research interests include electrical drive systems, power electronics, and electric vehicles. She can be contacted at email: vothanhha.ktd@utc.edu.vn.

Vo Quang Vinh 🆔 🔍 SC ◑ received the B.S degree in Control and Automation Engineering from Thai Nguyen University of Technology, Vietnam in 1995. The Master's degree from Hanoi University of Science and Technology, Vietnam in 1998, and the Ph.D. from Hanoi University of Science and Technology, Vietnam in 2004. He has worked in Faculty of Control and Automation, Electric Power University, Vietnam since 2011. Currently, Dr Vo Quang Vinh′s research interests are electrical drive and power electronics, control and automation. He can be contacted at email: vinhvq@epu.edu.vn.